


**Please cite the Published Version**

Burns, K, Ingram, IDV, Potgieter, JH  and Potgieter-Vermaak, S (2023) Synthesis and performance evaluation of novel soybean oil-based plasticisers for polyvinyl chloride (PVC). Journal of Applied Polymer Science. e54656-e54656. ISSN 0021-8995

**DOI:** <https://doi.org/10.1002/app.54656>

**Publisher:** Wiley

**Version:** Published Version

**Downloaded from:** <https://e-space.mmu.ac.uk/632568/>

**Usage rights:**  [Creative Commons: Attribution 4.0](https://creativecommons.org/licenses/by/4.0/)

**Additional Information:** This is an Open Access article published in Journal of Applied Polymer Science, by Wiley.

**Data Access Statement:** The raw data required to reproduce these findings are available to download from <https://doi.org/10.23634/MMU.00632240>.

**Enquiries:**

If you have questions about this document, contact [rsl@mmu.ac.uk](mailto:rsl@mmu.ac.uk). Please include the URL of the record in e-space. If you believe that your, or a third party's rights have been compromised through this document please see our Take Down policy (available from <https://www.mmu.ac.uk/library/using-the-library/policies-and-guidelines>)

# Synthesis and performance evaluation of novel soybean oil-based plasticisers for polyvinyl chloride (PVC)

Katharine Burns<sup>1</sup>  | Ian D. V. Ingram<sup>1</sup>  | Johannes H. Potgieter<sup>1,2</sup>  |  
Sanja Potgieter-Vermaak<sup>1</sup> 

<sup>1</sup>Department of Natural Sciences,  
Manchester Metropolitan University,  
Manchester, United Kingdom

<sup>2</sup>School of Chemical and Metallurgical  
Engineering, University of the  
Witwatersrand, PO Wits, South Africa

## Correspondence

Ian D. V. Ingram, Department of Natural  
Sciences, Manchester Metropolitan  
University, Chester Street, Manchester,  
M1 5GD, United Kingdom.  
Email: [i.ingram@mmu.ac.uk](mailto:i.ingram@mmu.ac.uk)

## Funding information

Alphagary Ltd.

## Abstract

Novel bio-based plasticisers for polyvinyl chloride (PVC) are a significant and growing area of interest. These compounds aim to replace toxic and petrochemical additives in commonly used plastic products. Plasticisers can comprise as much as 50% of the total mass of the PVC product. Epoxidised soybean oil (ESBO) is a commercially available bio-based plasticizer that is typically used at lower levels than traditional phthalates in PVC compounds because it does not show equivalent performance to existing phthalate plasticisers. Four derivatives of ESBO have been synthesized through reaction at the epoxide rings. These compounds have been evaluated in PVC formulations and compared to current petrochemical plasticisers, as well as ESBO. The product of methoxy polyethylene glycol and ESBO shows good plasticising ability, giving a PVC compound with higher tensile strength and elongation than dioctyl phthalate (DOP) and a lower glass transition temperature (T<sub>g</sub>) than with the use of ESBO.

## KEYWORDS

bio-based plasticizer, epoxidised soybean oil, phthalate, PVC, renewable

## 1 | INTRODUCTION

PVC (polyvinyl chloride) is used around the world in many different applications, owing to the wide variety of properties that can be obtained through the use of additives such as plasticisers.<sup>1</sup> Unplasticised PVC (U-PVC) is commonly used in construction, for products such as window frames and guttering, while plasticised PVC (pPVC) has uses in medical tubing, electrical insulation, toys and clothing (among others). Plasticisers create flexibility in polymers by increasing the free volume between the polymer chains, which allows the polymer to move and stretch more easily.<sup>2</sup> Plasticisers used in PVC

formulations typically contain a mixture of polar and non-polar groups. The polar groups (such as esters) provide noncovalent interactions with the polymer chain, while the non-polar groups (such as alkyl chains) increase the free volume and provide lubrication.<sup>2,3</sup>

The most commonly used plasticisers for PVC are phthalates (e.g., diethyl hexyl phthalate, DOP/DEHP, Figure 1) which are derived from oil and can exhibit toxic and harmful effects on the endocrine system, especially in children.<sup>2</sup> Many petrochemical alternatives to phthalates have been developed and commercialized, such as benzoates (sold under the Benzoflex<sup>®</sup> brand by Eastman, 4) and Hexamoll<sup>®</sup> DINCH (BASF, 3). The use of non-

This is an open access article under the terms of the [Creative Commons Attribution](https://creativecommons.org/licenses/by/4.0/) License, which permits use, distribution and reproduction in any medium, provided the original work is properly cited.

© 2023 The Authors. *Journal of Applied Polymer Science* published by Wiley Periodicals LLC.

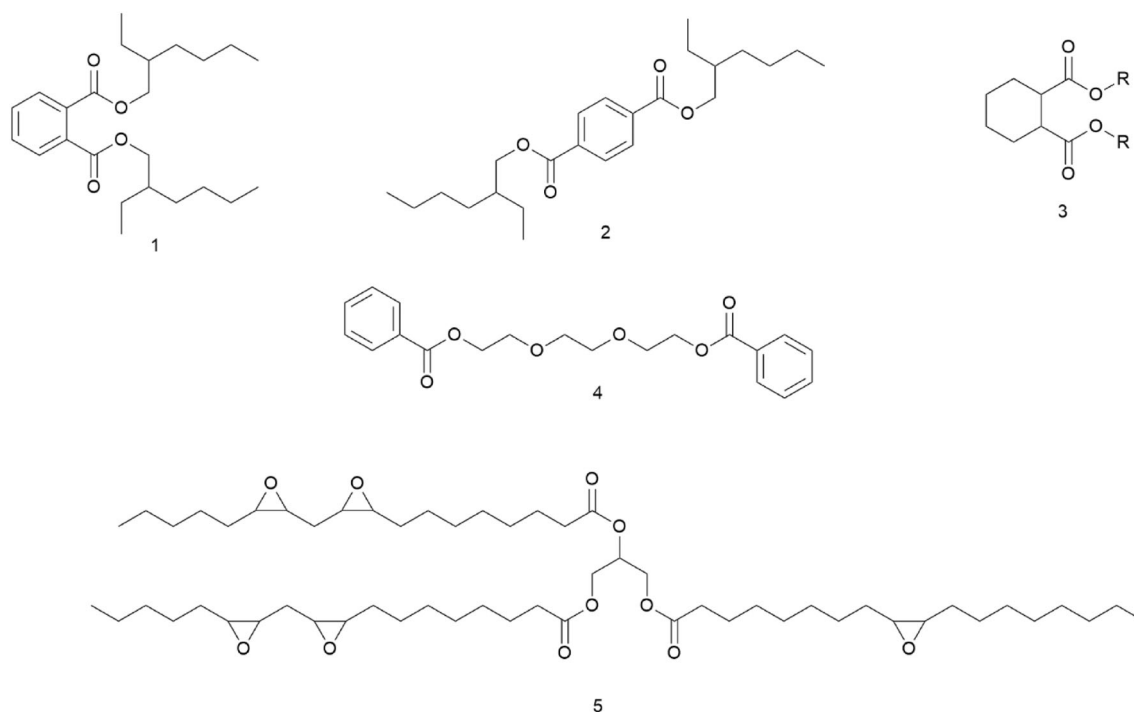


**FIGURE 1** Chemical structures of petrochemical plasticisers used in PVC formulations – diethylhexyl phthalate (1), diethylhexyl terephthalate (2), 1,2-cyclohexane dicarboxylates (3, such as DINCH, where R = isononyl), benzoates (4) and representative structure of epoxidised soybean oil (ESBO, 5).

phthalate plasticisers globally has continued to increase, from 12% in 2005 up to 35% in 2017.<sup>4</sup> Terephthalates (e.g., diethyl hexyl terephthalate, DOTP, **2**) are the para-isomers of phthalates and are widely used in PVC formulations. Despite the similarity in structure to phthalates, these compounds are non-toxic and approved for use in food-contact plastics and childcare items.<sup>5,6</sup> Plasticised PVC formulations typically contain 15–50% plasticizer and can even contain up to 1.8 times as much plasticizer as PVC resin.<sup>7</sup> As such, replacing petrochemical plasticisers with bio-based alternatives can have a significant impact on the sustainability of the PVC product.

Epoxidised soybean oil (ESBO, **5**) is often used at low levels in PVC formulation but is not sufficiently compatible with the polymer to be practical as a primary plasticizer.<sup>2,8</sup> The reactivity of the epoxide ring has been used to functionalize ESBO for a number of bio-based applications.<sup>9,10</sup> By attaching more polar bio-based chemical groups, the compatibility of ESBO with PVC could be improved, allowing for greater bio-based content in PVC products. A typical composition of soybean oil is 53% C18:2 (fatty acid chain length: unsaturation), 22% C18:1, 12% C16:0, 8% C18:3, 5% other, thus giving 4–5 epoxide groups in the resulting ESBO.<sup>11</sup>

The epoxide ring opening reaction of ESBO is well established with a range of nucleophiles such as alcohols, diols and amines, with reports going back as far as 1995.<sup>10,12,13</sup> These reactions have been used to produce

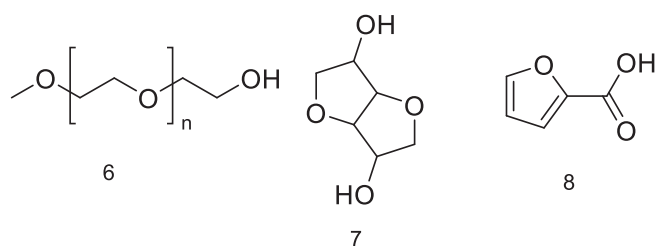


**FIGURE 2** Bio-based PEG-methyl ether (6), isosorbide (7) and 2-furoic acid (8) used to prepare modified ESBO plasticisers for PVC.

polyols for applications such as the synthesis of polyurethanes and other bio-based polymer alternatives.<sup>9,14,15</sup> The polyols can also be further functionalized by esterification reactions which can be used to introduce additional polar groups to the molecule.<sup>16</sup> Despite the utility of the epoxide ring as a target for synthetic modification, retaining some epoxide functionality could be desirable, due to the benefits to both compatibility and stability.<sup>17,18</sup> ESBO is often used as a heat stabilizer in PVC, as the epoxide ring scavenges the hydrochloric acid produced by PVC degradation. This prevents the acid from promoting further degradation of the PVC chain.<sup>2</sup>

The target compounds studied in this work aim to improve upon the compatibility between ESBO and PVC to develop a replacement for DOP in PVC formulations. As such, the success of the synthesized plasticisers will be

determined by the degree to which the resulting plasticizer replicates the performance of DOP when combined with PVC. The reactant molecules (Figure 2) were chosen to introduce more polarity into the structure of the plasticizer, thus increasing the intermolecular attraction between the plasticizer and the PVC polymer. Additionally, the ubiquitous phthalate plasticisers in part owe their compatibility to the aromatic ring in their structure, and the introduction of aromaticity into bio-based plasticisers intended to replace phthalates has therefore also been the subject of investigation.<sup>19</sup> In a computational analysis of a series of phthalate plasticisers, the aromatic ring was found to have the largest contribution towards the polymer-plasticizer interaction.<sup>20</sup> Furans can be produced from biomass and are a significant area of renewable chemistry, and importantly are a much more scalable and accessible source of bio-based aromaticity than benzene derivatives which (with some exceptions) are less available from biomass.<sup>21</sup> As such, one target molecule investigated here is the ester of 2-furoic acid (8), with the aim of introducing aromaticity into the ESBO derivative structure. Furoic acid is produced by the oxidation of furfural, which has been produced commercially from biomass for decades.<sup>22</sup> Isosorbide is derived from natural sugars and has shown promise as a component of a bio-based plasticizer for PVC in the form of a diester.<sup>23</sup> Polyethylene glycol and compounds thereof have also been investigated in PVC plasticisation and have the interesting property of both adding a branched, higher-volume morphology to the ESBO backbone, as well as additional polarity.<sup>24–26</sup> In this study, we prepare four different bio-based ESBO derivatives, and evaluate their performance as plasticisers for PVC against both ESBO itself and traditional petrochemical plasticisers DOP and DOTP. A successful bio-based plasticizer will show plasticising properties that are more similar to the petrochemical plasticisers DOP and DOTP, relative to the ESBO starting material.

## 2 | EXPERIMENTAL

### 2.1 | Materials

PVC resin (suspension grade, K70), barium-zinc based liquid heat stabilizer and plasticisers (DOP, DOTP and ESBO, industrial grade) were provided by Alphagary Ltd. Additionally, chemicals used were magnesium sulfate (Laboratory reagent grade, Fisher Scientific), methoxypolyethylene glycol (average molecular weight 350, Alfa Aesar), p-toluene sulfonic acid (99%, Acros Organics), zinc trifluoromethane sulfonate (98%, Acros Organics), methanol ( $\geq 99.9\%$ , Fisher Scientific), D-isosorbide

(98%, Alfa Aesar), 2-furoic acid (98%, Acros Organics), THF (Fisher Scientific, PureSolv purification system), chloroform (Fisher Scientific, >99% lab reagent grade), DCM (Fisher Scientific, >99% lab reagent grade), deuterated chloroform (Sigma Aldrich), diethyl ether (Fisher Scientific, laboratory reagent grade), sodium hydrogen carbonate (Fisher Scientific Laboratory reagent grade), toluene (Fisher Scientific, PureSolv purification system).

### 2.2 | Characterization

$^1\text{H}$ ,  $^{13}\text{C}$ , and DOSY NMR were carried out on a JEOL ECS 400 MHz FT-NMR. Deuterated chloroform was used as solvent and spectra were referenced by the solvent peak. FTIR spectra were measured on a Perkin Elmer Spectrum Two ( $4000\text{--}400\text{ cm}^{-1}$ , resolution  $4\text{ cm}^{-1}$ , 16 scans). These techniques were used to analyze the synthetic products formed.

### 2.3 | Synthesis of novel plasticisers

The reaction of the ESBO epoxide functionality with alcohols was carried out under acidic conditions. The catalyst was chosen to prevent transesterification reactions from occurring. As ESBO is not a single molecule and has approximately 5 possible reaction sites per molecule, calculating precise yields is unlikely to give valid results. As such, yields are expressed by mass. Reaction schemes and product structures are also shown as simplified representations due to the complex structure of ESBO – each triglyceride may contain fatty acids of variable composition as detailed previously, with 0, 1 or 2 epoxide groups present. Furthermore, each nucleophilic attack at an epoxide can occur at either carbon of the epoxide ring, leading to numerous possible products. Assignments and structures are presented in [supplementary information](#).

### 2.4 | Synthesis of methyl ether ESBO polyol (MEEP, 9)

ESBO (53.67 g) was reacted with excess methanol (90 mL) with zinc triflate catalyst (0.25 g). The reaction mixture was stirred at reflux ( $65^\circ\text{C}$ ) under argon for 20 h. The reaction mixture was cooled to room temperature and the solvent removed in vacuo. The crude product was dissolved in chloroform (50 mL), washed with 1 M sodium bicarbonate solution (50 mL) and deionized water (2 x 50 mL). The organic fraction was dried over magnesium sulfate and concentrated in vacuo to give a yellow oil (53.02 g).

$\delta$ H (400 MHz,  $\text{CDCl}_3$ ) 5.26 (m), 4.29 (dd,  $J = 11.8$ , 4.2 Hz), 4.14 (dd,  $J = 11.9$ , 5.9 Hz), 3.52–3.42 (m), 3.41 (s), 2.99 (q,  $J = 5.7$  Hz) 2.31 (t,  $J = 7.6$  Hz), 1.61–1.26 (m), 0.88 (m).

$\delta$ C (101 MHz,  $\text{CDCl}_3$ ) 173.43, 173.01, 84.46, 72.74, 68.98, 62.21, 58.25, 56.75, 50.97, 39.14, 38.83, 38.05, 34.30, 33.63, 33.51, 32.19, 32.05, 32.01, 30.11, 30.02, 29.88, 29.82, 29.60, 29.49, 29.40, 29.24, 29.18, 26.11, 25.90, 25.16, 24.98, 24.93, 22.81, 22.74, 14.25, 14.20.

$\nu_{\text{max}}/\text{cm}^{-1}$  3456, 2926, 2855, 1742  $\text{cm}^{-1}$ .

## 2.5 | Synthesis of ESBO-mPEG ether polyol (mPEG-ESBO, 10)

mPEG (methoxy polyethylene glycol, 52.15 g, 0.15 mol) of average molecular weight 350 Da was reacted with ESBO (15.08 g, 0.015 mol) and zinc triflate catalyst (0.022 g, 0.06 mmol) at 150°C under argon with stirring for 2 h. The reaction mixture was cooled to room temperature and triturated with deionized water (3 x 50 mL). The resulting yellow oil was dissolved in chloroform, dried over anhydrous magnesium sulfate, and concentrated in vacuo, giving a mass of 15.32 g.

$\delta$ H (400 MHz,  $\text{CDCl}_3$ ) 5.25 (m), 4.29 (m), 3.65 (s), 3.55 (m), 3.38 (s), 2.31 (t,  $J = 7.6$  Hz), 1.76–1.13 (m), 0.88 (m).

$\delta$ C (101 MHz,  $\text{CDCl}_3$ ) 173.36, 172.95, 104.95, 104.88, 72.71, 72.02, 70.65, 70.38, 68.96, 62.18, 61.79, 59.13, 42.94, 42.85, 42.80, 36.10, 34.25, 34.14, 34.08, 32.02, 31.96, 31.91, 31.69, 31.51, 29.79, 29.75, 29.57, 29.46, 29.37, 29.21, 29.16, 29.10, 28.98, 28.17, 28.12, 27.91, 24.95, 24.90, 23.98, 23.89, 23.83, 22.78, 22.67, 22.52, 14.22.

$\nu_{\text{max}}/\text{cm}^{-1}$  3476, 2925, 2856, 1742  $\text{cm}^{-1}$ .

## 2.6 | Synthesis of furoic acid ester of methoxylated ESBO (MEFE, 11)

Methyl Ether ESBO Polyol (MEEP, 10.00 g) was reacted with furoic acid (6.28 g) in dry toluene (100 mL) with PTSA catalyst (0.964 g) in a round bottomed flask with a Dean-Stark condenser trap. The mixture was stirred at reflux (110°C) for 18 h and cooled to room temperature and the solvent removed in vacuo. The crude product was dissolved in chloroform (50 mL), washed with 1 M sodium bicarbonate solution (50 mL) and deionized water (2 x 50 mL). The organic fraction was dried over magnesium sulfate and concentrated in vacuo to give a brown oil (11.21 g).

$\delta$ H (400 MHz,  $\text{CDCl}_3$ ) 7.88–7.49 (m), 6.51 (m), 5.25 (m), 4.34–4.08 (m), 3.41 (s), 2.99 (m), 2.35 (s), 2.31 (t,  $J = 7.6$  Hz), 2.09 (s), 1.72–1.16 (m), 0.87 (t,  $J = 6.9$  Hz).

$\delta$ C (101 MHz,  $\text{CDCl}_3$ ) 173.42, 130.14, 129.44, 129.17, 128.36, 128.15, 126.67, 125.43, 111.93, 68.99, 65.20, 62.21, 34.18, 32.06, 29.84, 29.79, 29.64, 29.50, 29.41, 29.25, 25.82, 24.97, 22.82, 21.59, 14.26, 14.17.

$\nu_{\text{max}}/\text{cm}^{-1}$  3020, 2927, 2856, 1735, 1661  $\text{cm}^{-1}$ .

## 2.7 | Synthesis of Isosorbide ether ESBO polyol (IEEP, 12)

ESBO (15.01 g) was reacted with an excess of isosorbide (33.83 g) in THF (175 mL) with zinc triflate catalyst (0.279 g). The chemicals were dissolved in THF and dried with excess magnesium sulfate, then filtered into a dry round bottomed flask. The mixture was heated to reflux under argon for 20 h with stirring. The reaction mixture was cooled to room temperature and the solvent removed in vacuo. The crude product was dissolved in diethyl ether (50 mL), washed with 1 M sodium bicarbonate solution (50 mL) and deionized water (2 x 50 mL). The organic fraction was dried over magnesium sulfate and concentrated in vacuo to give a yellow oil (19.33 g).

$\delta$ H (400 MHz,  $\text{CDCl}_3$ ) 5.25 (m), 4.7–4.4 (m), 4.21 (ddd,  $J = 59.9$ , 11.7, 5.1 Hz), 4.05–3.53(m), 3.49–3.37 (m), 2.38 (t,  $J = 7.4$  Hz), 2.31 (t,  $J = 7.6$  Hz), 1.70–1.20 (m), 0.88 (m).

$\delta$ C (101 MHz,  $\text{CDCl}_3$ ) 173.46, 104.91, 70.76, 68.98, 62.22, 43.01, 34.29, 34.14, 32.06, 29.84, 29.80, 29.61, 29.51, 29.41, 29.22, 28.18, 26.61, 24.98, 24.02, 22.81, 22.73, 14.28.

$\nu_{\text{max}}/\text{cm}^{-1}$  3457, 2926, 2855, 1741  $\text{cm}^{-1}$ .

## 2.8 | Evaluation of novel plasticisers in PVC compounds

### 2.8.1 | Solvent casting of plasticised films

Plasticizer (2.5 g) was dissolved in 50 mL THF in a 100 mL round bottomed flask with stirrer bar. 0.05  $\mu\text{L}$  liquid barium-zinc stabilizer was added with stirring, followed by 5 g PVC resin (K70 suspension resin). A condenser was attached, and the mixture was heated to reflux (66°C) under argon for 2 hours until the polymer was fully dissolved. The mixture was allowed to cool to room temperature and then poured into a dry glass petri dish and loosely covered to allow gradual evaporation of the THF for 7 days.

The films were removed from the petri dishes and dried under vacuum at 40°C for 2 hours to remove residual THF. This was shown to be sufficient for the removal of THF by TGA analysis which did not show a mass loss step that could be attributed to THF evaporation.

This method does not replicate the methods of PVC plasticisation used in the PVC industry, however such methods (extrusion, 2-roll milling) would require greater quantities of plasticizer than were available in this study.

### 2.8.2 | Tensile testing

For the tensile properties testing, 1 mm thickness plaques were prepared using a heated hydraulic press. The cast films were placed in a steel mold which was subjected to 200 bar at 160°C for 4 min and cooled under pressure. Dumbbell shaped pieces in accordance with BS EN ISO 527-2:2012 (Type 5A) were cut from the molded sheets. The thickness of the central portion was measured and recorded. Five test pieces were prepared for each plasticised PVC formulation.

The tensile properties of the molded films were tested in accordance with BS EN ISO 527-1:2019 using a Hounsfield H10KS UTM equipped with a 1000 N load cell and laser extensometer. The speed of the moving grip was set to 100 mm/min. Load and extension were measured, and stress and strain calculated from the sample dimensions.

### 2.8.3 | Dynamic mechanical analysis

DMA was used to investigate the low temperature properties of the samples. This analysis was carried out using a Perkin Elmer DMA 8000 in tensile mode on samples of dimension 6 x 20 mm cut directly from the cast films. Sample thicknesses were measured to 0.01 mm and were approximately 1 mm. Samples were tested from -130 to 70°C at a rate of 5°C/min. The samples were exposed to an oscillating strain of 0.5 mm at a frequency of 1 Hz.

### 2.8.4 | Thermogravimetric analysis

Samples of the novel plasticisers and plasticised films were tested by TGA using a Mettler Toledo TGA 1. Samples of approximately 15 mg were weighed into aluminium pans (plasticisers) or alumina crucibles (PVC samples) and heated at 20°C/min to 600°C (plasticisers) or 1000°C (PVC samples) under nitrogen.

### 2.8.5 | Scanning electron microscopy

PVC samples were cold fractured under liquid nitrogen. The fracture surfaces were sputter coated with gold/palladium (10 nm thickness) and examined by SEM

(Zeiss Supra 40VP) at 5000–20,000× magnification, 2 kV acceleration voltage, to investigate the internal structure.

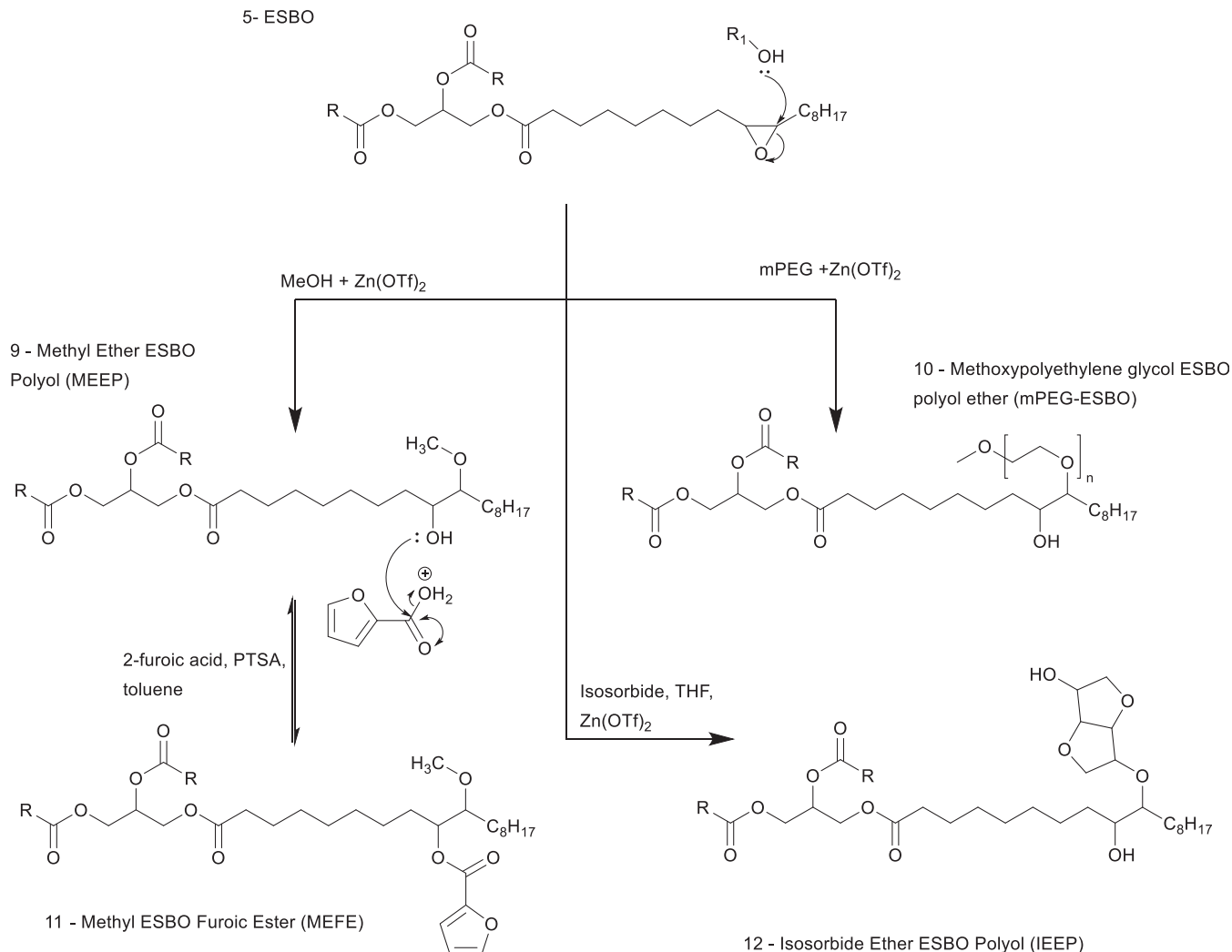
## 3 | RESULTS AND DISCUSSION

The reactions were carried out as presented in Scheme 1. The synthesis of novel plasticisers was monitored primarily by <sup>1</sup>H NMR. As ESBO itself is a mixture with multiple possible reaction sites, the resulting products were themselves mixtures. As such, options for purification of the products were limited since typical routes such as column chromatography were unsuitable.

Methyl ether ESBO polyol (MEEP, **9**) has been synthesized in previous works<sup>9,27</sup> as a precursor for polyurethane synthesis and was primarily prepared here as an intermediate. Zinc triflate, PTSA and sulfuric acid were all evaluated for use as catalysts in the ring opening reaction with methanol based on their use in similar works,<sup>9,14</sup> but zinc triflate was chosen as this gave the greatest conversion and did not lead to significant transesterification, which was observed when sulfuric acid or higher levels of PTSA were used (Figure 3).

The structure was confirmed with FTIR-ATR spectroscopy which showed the broad alcohol O-H stretch at 3400–3500 cm<sup>-1</sup>, as well as a reduction in the epoxide double peak (828 and 847 cm<sup>-1</sup>). As both ESBO and mPEG are mixtures, the resulting product will be a statistical mixture of composition and so precise structural determination is not possible. In the case of mPEG-ESBO, the terminal methyl group (3.4 ppm) was used to determine the progress of the reaction. In the final product, the methyl group was measured as 4.85 protons, indicating that on average each molecule of ESBO has reacted with 1–2 mPEG molecules. An excess of mPEG was used to ensure the greatest possible reaction of the epoxide rings. Methyl capped PEG was used to prevent crosslinking between ESBO molecules, as uncapped PEGs have two alcohol functionalities that could both react with epoxide rings. While isosorbide is also a diol with the potential to cause crosslinking, the two alcohol groups exhibit different reactivities. One alcohol group is in an endo-position that leads to hydrogen bonding with the furan ring, while the other alcohol group is in an exo-position and so is significantly more available for reaction.<sup>28</sup>

Purification was first carried out by dissolving the reaction mixture in chloroform and washing with water. However, this did not remove the residual mPEG. This was noted by <sup>1</sup>H NMR as integration of the peak corresponding to the terminal methyl of mPEG gave an equivalent of 12 mPEG chains per ESBO molecule despite the theoretical maximum number of epoxide sites being 5–6.



**SCHEME 1** Reaction scheme showing the synthesis routes for four bio-based derivatives of ESBO, 9- Methyl Ether ESBO Polyol (MEEP), 10- methoxy polyethylene glycol ESBO polyol ether (mPEG-ESBO), 11- Methoxylated ESBO Furoic Ester (MEFE), 12- Isosorbide Ether ESBO Polyol (IEEP).

Purification was instead carried out by trituration in water. The composition of the resulting product was confirmed by Diffusion-Ordered NMR Spectroscopy (DOSY). DOSY can be used to determine the composition of samples by separating the <sup>1</sup>H-NMR signals based on the diffusion properties of the molecules. Comparison of a mixture of ESBO and mPEG with the reaction product showed the difference following reaction. The two components are separated by their diffusion behavior in Figure 4, while Figure 5 shows a single diffusion coefficient, indicating that the product has been formed. FTIR-ATR also indicated that the product was formed, due to an alcohol O-H stretch at 3485 cm<sup>-1</sup>, reduction in epoxide (828 and 847 cm<sup>-1</sup>) and a peak at 1108 cm<sup>-1</sup> corresponding to the C-O-C asymmetric stretch of the ether groups.

In the synthesis of isosorbide ether ESBO polyol (IEEP, **12**), initial reactions showed a disappearance of

the epoxide ring signals by NMR, without new signals appearing which would correspond to the isosorbide structure. It was thought that this could be due to moisture and so all reactants were dried over magnesium sulfate prior to reaction and dry solvent was used. <sup>1</sup>H NMR peaks consistent with isosorbide were observed in the region 4–3.5 ppm, and the reaction was confirmed by DOSY NMR (Figure 6), which confirmed that the isosorbide was attached to ESBO, and FTIR, which showed alcohol formation, and hence conversion of epoxides, by the O-H stretch at 3452 cm<sup>-1</sup>.

The esterification of the alcohol groups formed by epoxide ring opening in MEEP (**9**) was attempted with furoic acid to introduce aromaticity into the plasticizer structure. Initial reaction attempts using a single vessel were unsuccessful, and so a Dean-Stark apparatus was used to remove water formed by the reaction. By using

this method, methoxylated ESBO furoic ester (MEFE, **11**) was produced. The MEFE product **11** was confirmed by  $^1\text{H}$  NMR, which showed peaks corresponding to the furan ring at 7.8, 7.2 and 6.5 ppm. DOSY analysis showed a single diffusion behavior confirming that the furan

signals were attached to the larger molecule and FTIR showed the inclusion of an  $\text{sp}^2$  C-H stretch at  $3019\text{ cm}^{-1}$  as well as the disappearance of the O-H stretch observed in MEEP **9** which confirms that the alcohol group has reacted.

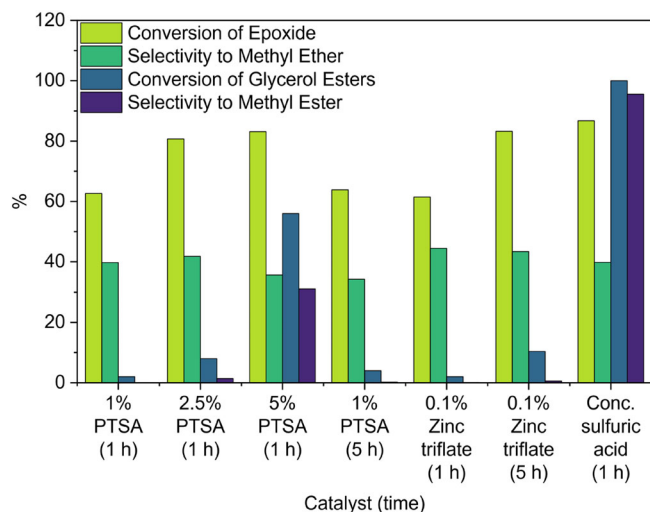


**FIGURE 3** Catalyst comparison for the methoxylation of ESBO measured by  $^1\text{H}$  NMR, showing conversion and selectivity of epoxide to methyl ether and glycerol esters to methyl esters (calculations listed in ESI). [Color figure can be viewed at [wileyonlinelibrary.com](http://wileyonlinelibrary.com)]

### 3.1 | Tensile testing

The tensile elongation and stress at the ultimate breakpoint for all samples are shown in Figure 7, and values including 100% modulus are presented in Table 1. The plasticised PVC films prepared by solvent casting were compression molded prior to tensile testing to give an even sample thickness throughout. However, both MEEP **9** and IEEP **12** showed delamination of the molded PVC samples, where the material did not fuse together when molded and instead separated into layers. This is an indication of poor compatibility, as delamination can be caused by plasticizer exudation which forms an oily layer on the surface, preventing fusion.

Tensile testing of flexible PVC samples typically shows a trend of increasing elongation and decreasing tensile stress at breakpoint with higher plasticisation. This is demonstrated with the three commercial plasticisers – DOP is known to be a more efficient plasticizer than DOTP (giving a softer product at the same weight percentage)

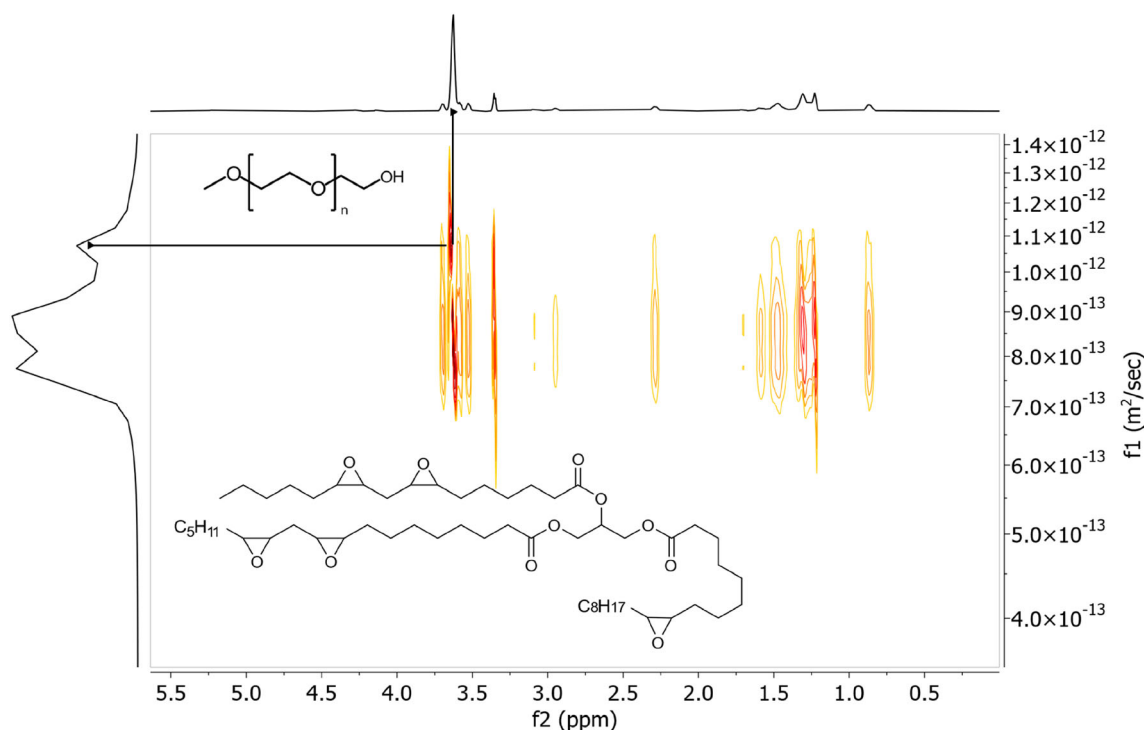


**FIGURE 4** DOSY NMR for a mixture of ESBO and mPEG showing the separation of the signals for the components. [Color figure can be viewed at [wileyonlinelibrary.com](http://wileyonlinelibrary.com)]



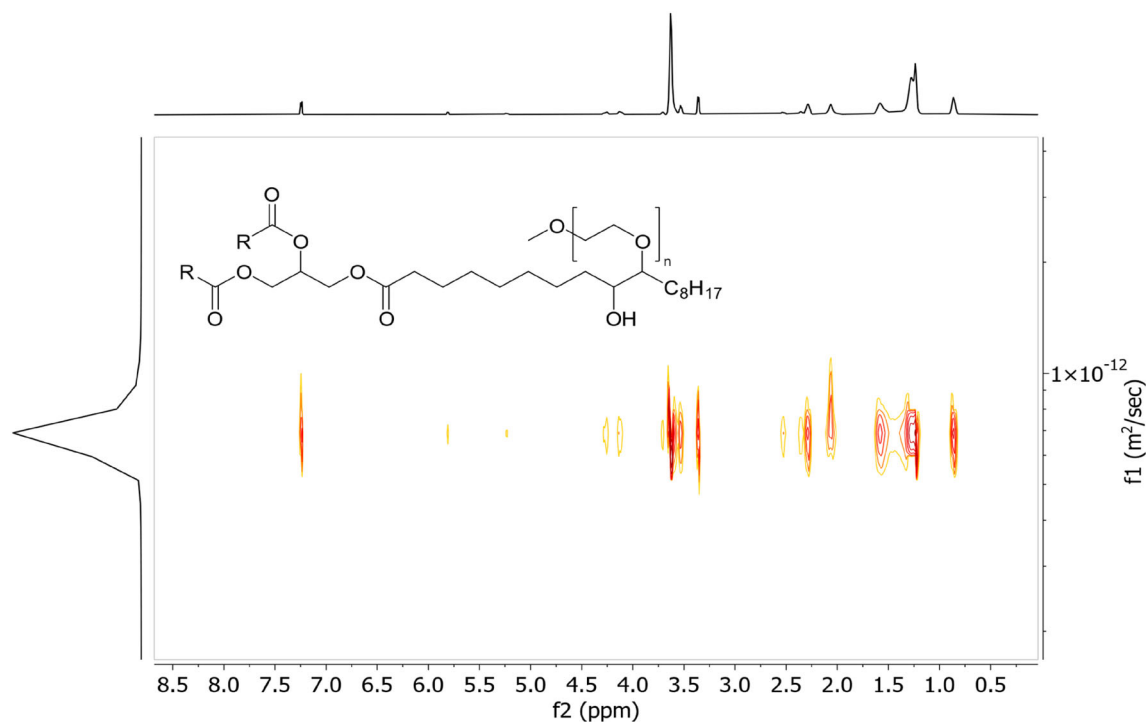


**FIGURE 5** DOSY NMR for the product of ESBO and mPEG (mPEG-ESBO **10**) showing a single diffusion behavior, indicating that the reaction has occurred. [Color figure can be viewed at [wileyonlinelibrary.com](http://wileyonlinelibrary.com)]

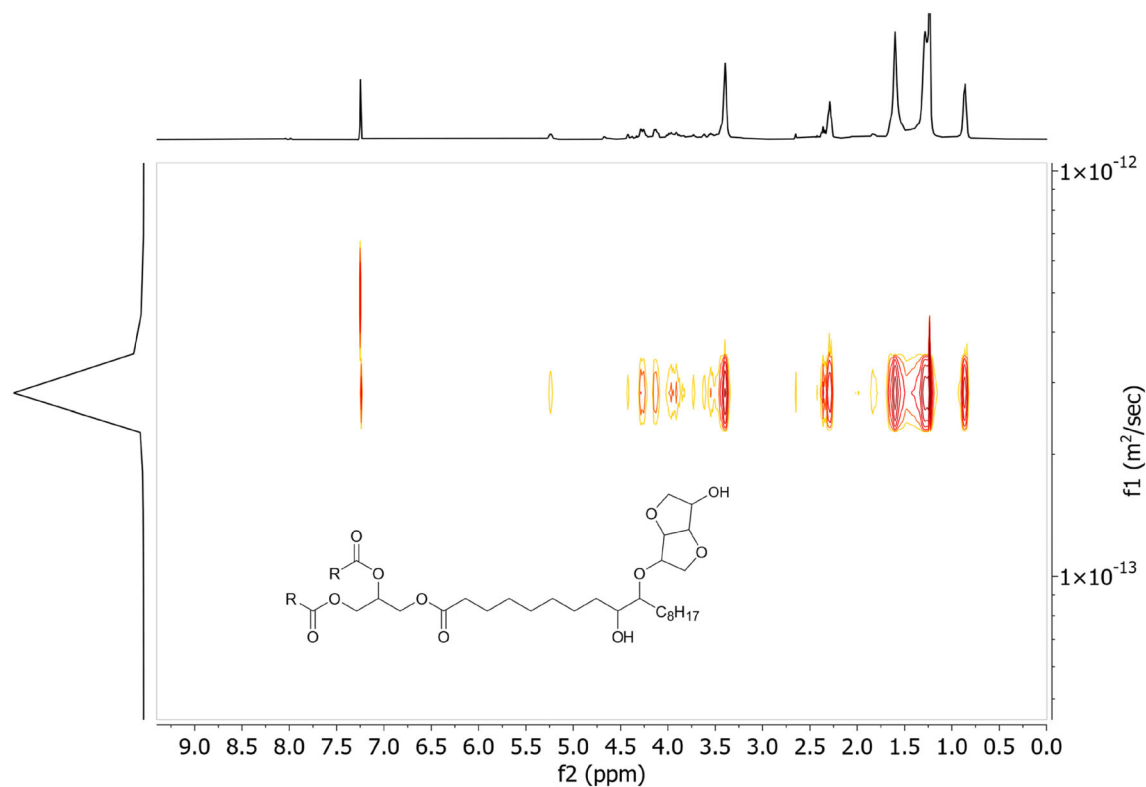


**FIGURE 6** DOSY NMR of IEEP (product of ESBO and isosorbide) showing a single diffusion behavior, indicating that all peaks are from the same molecule. [Color figure can be viewed at [wileyonlinelibrary.com](http://wileyonlinelibrary.com)]

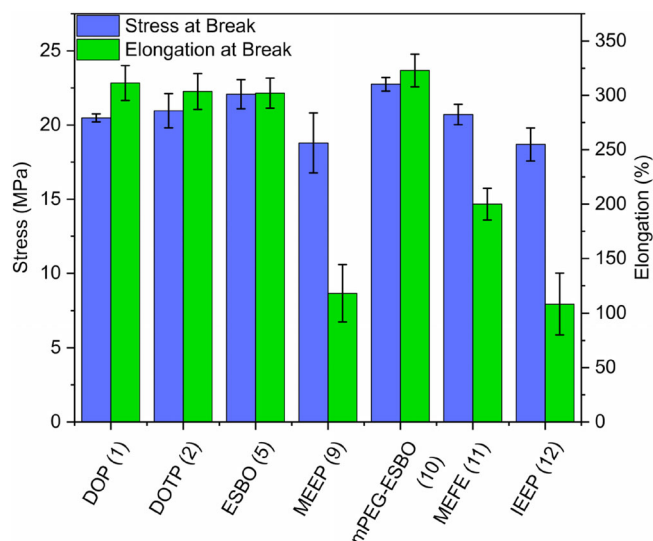


**FIGURE 7** Tensile Stress and Elongation at breakpoint for PVC samples produced with commercial and novel plasticisers. [Color figure can be viewed at [wileyonlinelibrary.com](https://onlinelibrary.wiley.com/doi/10.1002/app.54656)]

**TABLE 1** 100% Tensile Modulus, Tensile Stress and Elongation at breakpoint for the plasticised PVC samples.

| Plasticizer    | 100% modulus (MPa) | Stress at breakpoint (MPa) | Elongation at breakpoint (%) |
|----------------|--------------------|----------------------------|------------------------------|
| DOP (1)        | 10.3               | 20.5                       | 311.4                        |
| DOTP (2)       | 11.9               | 21.0                       | 303.6                        |
| ESBO (5)       | 12.75              | 22.1                       | 302.0                        |
| MEEP (9)       | 14.6               | 18.8                       | 118.2                        |
| mPEG-ESBO (10) | 12.6               | 22.8                       | 322.9                        |
| MEFE (11)      | 16.7               | 20.7                       | 200.0                        |
| IEEP (12)      | 8.4                | 18.7                       | 108.3                        |

and correspondingly DOP shows greater elongation and lower stress at breakpoint than DOTP or ESBO.

The mPEG-ESBO **10** product shows the highest elongation at breakpoint and tensile stress at breakpoint of all samples, which indicates that this new bio-based plasticizer gives greater strength and flexibility to the PVC product than the commercial plasticisers.

The other synthesized plasticisers show signs of less effective plasticisation, with lower stress and elongation at break than the commercial plasticisers. This indicates that these plasticisers do not as effectively lubricate the polymer chains to move within the polymer matrix and allow the test pieces to elongate under load. In fact, the stress-strain curves for the novel plasticisers show very different behavior for MEEP **9**, MEFE **11** and IEEP **12** as shown in Figure 8. mPEG-ESBO **10** is the only one of our

bio-based plasticisers that gives a similar profile of stress-strain behavior to the commercial PVC plasticisers. These samples displayed ductile behavior prior to break, with no necking of the sample, followed by a brittle fracture as indicated by SEM images ([supplemental data](#)). The other novel plasticisers also show ductile deformation behavior; however, this was followed by an early yield point leading to ‘necking’ of the sample. This necking creates a region of very high stress as the cross-section narrows, and thus leads to early fracture with low elongation and stress at breaking point. The fracture surfaces of these samples indicate a combination of brittle and ductile behavior.

### 3.2 | Dynamic mechanical analysis

DMA was used to measure the response of the plasticised samples to an oscillating deformation over a temperature range. The glass transition temperature  $T_g$  of the material can be determined by the point at which the response changes from ‘glassy’ elastic behavior to ‘rubbery’ inelastic behavior. The loss modulus is a measure of the inelastic component of the material response. The effect of a plasticizer on the glass transition temperature of PVC is a common metric of plasticizer compatibility and performance.<sup>29–31</sup> Effective plasticisation leads to a lower  $T_g$ , while poor plasticisation can also give rise to phase separation which is shown through multiple or poorly defined glass transitions.

The  $T_g$  of plasticised PVC samples was determined by the peak of the loss modulus (Figure 9, see supplementary information for plots of storage modulus and tan delta). All novel compounds gave a lower  $T_g$  than ESBO, however the loss modulus peaks were generally broader and less well defined. IEEP showed the lowest average  $T_g$ , but the peak width was more than double that of ESBO (FWHM of 82.2°C compared with 39.7°C). The peak width of mPEG-ESBO **10** was also broad, despite this plasticizer generally showing good performance in other material properties. It is possible that this could be due to the broader composition of this product than the other novel plasticisers, as both ESBO and mPEG starting materials are composed of mixtures of chain lengths and molecular weights.

### 3.3 | Thermogravimetric analysis

Thermogravimetric analysis was carried out on the plasticisers and plasticised PVC samples. For the plasticisers alone, the data shows the volatility of the plasticizer, while for the plasticised PVC samples this technique also

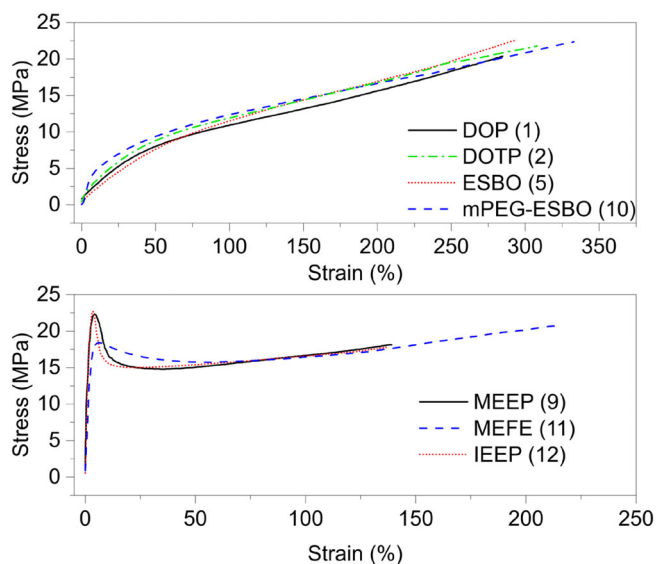


**FIGURE 8** Stress-strain curves for tensile elongation of plasticised PVC samples. [Color figure can be viewed at [wileyonlinelibrary.com](http://wileyonlinelibrary.com)]

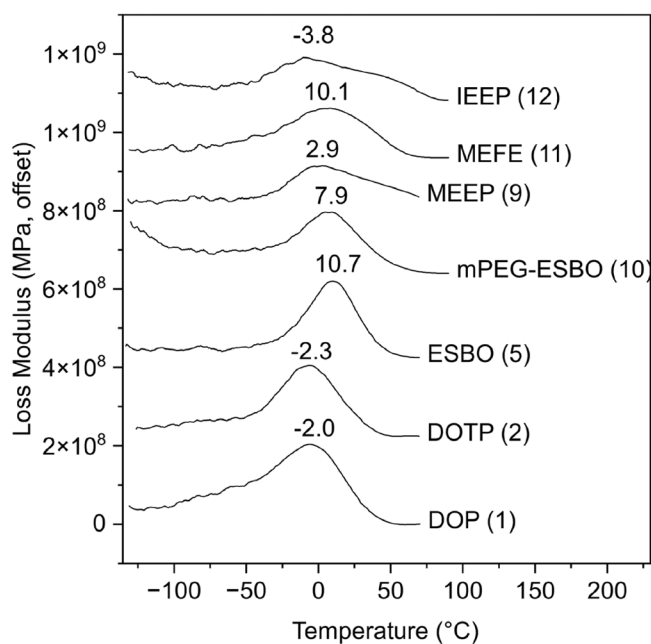


**FIGURE 9** Loss modulus against sample temperature by DMA for samples of plasticised PVC prepared by solvent casting.

shows the effect of the plasticizer on the degradation of the PVC. Figure 10 shows the mass loss of the plasticisers by TGA. All of the modified-ESBO plasticisers showed an earlier onset of evaporation than ESBO itself. The mass loss also progressed in multiple distinct steps for MEEP 9, MEFE 11 and IEEP 12, whereas for mPEG-ESBO 10 the mass loss occurred gradually throughout the experiment. The temperatures of 5% and 50% mass loss ( $T_{95\%}$  and  $T_{50\%}$ ) are presented in Table 2.

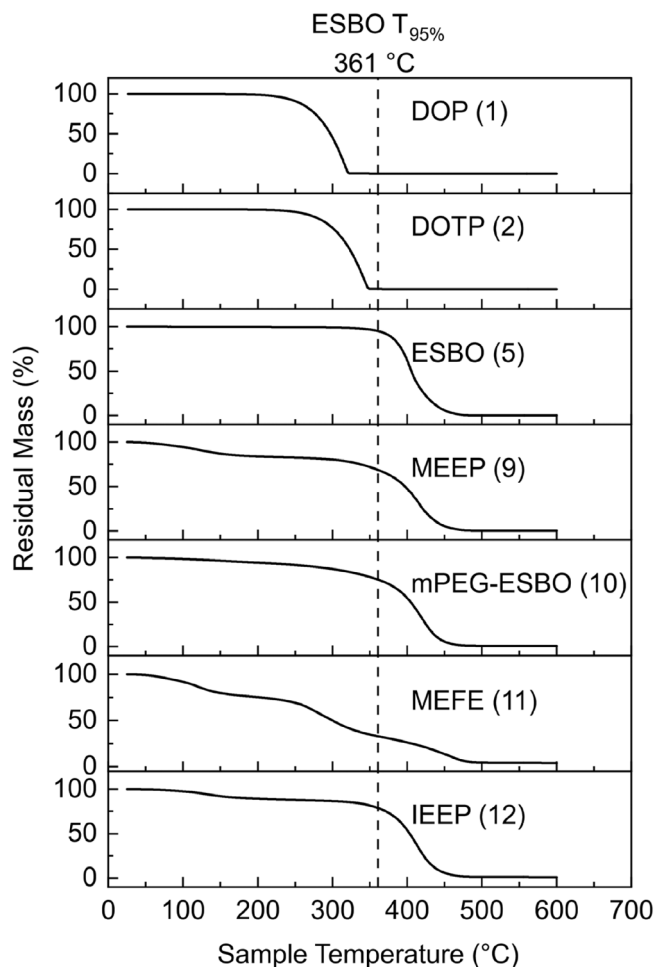


**FIGURE 10** Thermogravimetric analysis of commercial and modified-ESBO plasticisers.

**TABLE 2** Temperature of 5% and 50% mass loss for plasticisers by TGA.

| Plasticizer    | $T_{95\%}$ | $T_{50\%}$ |
|----------------|------------|------------|
| DOP (1)        | 236        | 297        |
| DOTP (2)       | 260        | 323        |
| ESBO (5)       | 361        | 406        |
| mPEG-ESBO (10) | 185        | 405        |
| MEEP (9)       | 95         | 397        |
| MEFE (11)      | 82         | 300        |
| IEEP (12)      | 126        | 403        |

MEFE showed the earliest onset of mass loss, losing 5% by 82°C. The other novel plasticisers showed a lower  $T_{95\%}$  than ESBO, but comparable  $T_{50\%}$  values. As such, while the major component of these plasticisers appears to have similar volatility to ESBO, these also contain more volatile or unstable minor components.

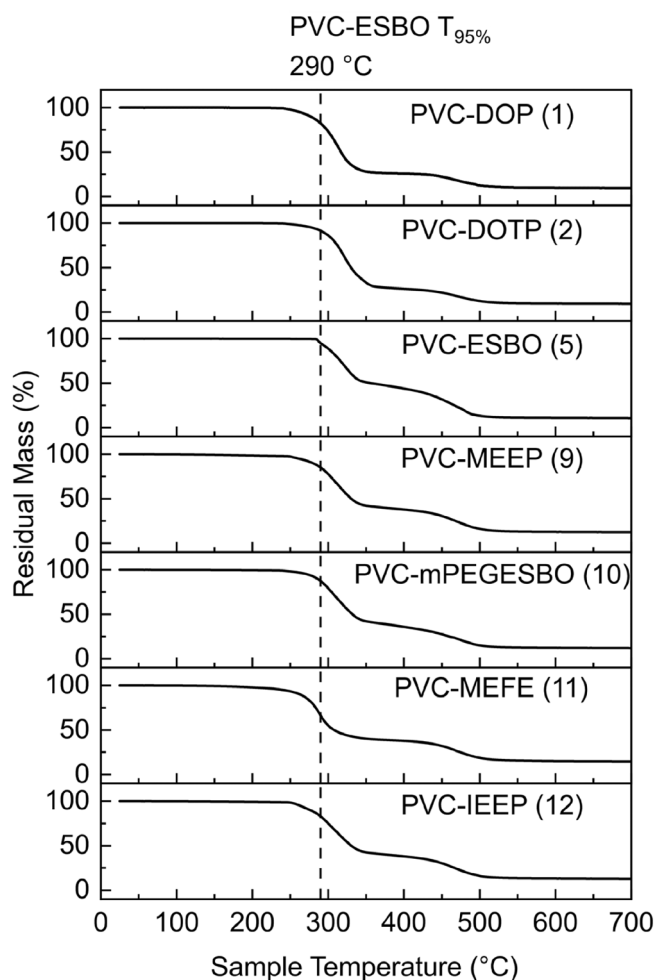


FIGURE 11 Thermogravimetric analysis of plasticised PVC samples.

The TGA results for the plasticised PVC samples (Figure 11) show the effect of the plasticizer on the decomposition of PVC. These data also confirm that there is no significant residual THF present in the samples, as this would be notable by a mass loss step at approximately 65°C. All samples contained the same amount of liquid heat stabilizer additive. PVC decomposition occurs in two stages – first dehydrochlorination, forming conjugated polyenes and hydrochloric acid, followed by cyclisation to form benzene and other aromatic compounds.<sup>32</sup> The epoxide rings in ESBO react with chloride ions that are released during PVC decomposition.<sup>33</sup> This slows the degradation as the hydrochloric acid produced by the PVC decomposition acts as a catalyst for this decomposition. Epoxides can also replace labile chlorine atoms to form  $\alpha$ -chloro-ethers which prevents the dehydrochlorination reaction.<sup>33</sup> Two main mass loss steps were identified for all samples of plasticised PVC. As well as the PVC decomposition, these steps will also include volatilization and decomposition of the plasticizer, however

these processes could not be specifically and separately identified in the data. The onset temperature and percentage mass loss for the two steps is presented in Table 3. Onset temperatures were calculated by the intersection of tangents using the Mettler Toledo STARE Evaluation software.

The effect of ESBO on PVC decomposition is observable in the Step 1 mass loss. PVC-DOP and PVC-DOTP lose 73.9 and 73.7% of the total sample mass in this step, while PVC-ESBO loses only 54.1%. This is likely to be a combination of the reduction in dehydrochlorination as described, as well as the lower volatility of ESBO. All of the synthesized plasticizer samples retained some degree of this behavior, with mass loss ranging from 61.2% to 63.2%. This suggests that unreacted epoxide rings remain present in the compounds and may function as PVC stabilizers. <sup>1</sup>H NMR measurement of the epoxide signals in the novel plasticisers supports this, as some residual epoxide could be detected in all products.

However, the onsets of degradation in the samples prepared with the synthesized plasticisers are lower than with ESBO, showing that these plasticisers produced from ESBO do not stabilize the PVC to the same extent. This is expected, as the epoxide functionality that provides the stabilization effect is also the functionality that has been exploited in this synthesis. As Table 3 shows, the  $T_{95\%}$  for the novel plasticisers are comparable to the petrochemical plasticisers (with the exception of MEFE 11 which is somewhat lower) and so these plasticisers are suitably non-volatile for use in PVC compounds. mPEG-ESBO 10 shows the highest  $T_{95\%}$  of the ESBO-derived plasticisers.

### 3.4 | Scanning electron microscopy

SEM images of plasticised PVC samples are shown in Figure 12. The samples containing commercial plasticisers DOP 1 and ESBO 5 both show smooth planes in the fractured surfaces, indicating good solvation of the PVC grains. There is no evidence of phase separation identifiable in these images. PVC-MEEP 9 shows mainly smooth planes with some inclusions observed. PVC-mPEG-ESBO 10 is the most similar in appearance to the commercial plasticisers, however there are some features visible that appear fibrous. Features of this sort are sometimes seen as a result of localized crystallization of the plasticizer, however this phenomenon is difficult to characterize and was not investigated further. PVC-MEFE 11 displays a very uneven microstructure, with large irregular regions visible. The surface of the fracture planes also appears to be rougher than in PVC-DOP or PVC-ESBO. PVC-IEEP 12 also shows signs of roughness on the fracture planes

TABLE 3 Thermogravimetric analysis of plasticised PVC samples.

| Plasticizer    | Step 1 onset (°C) | Step 1 mass loss (%) | Step 2 onset (°C) | Step 2 mass loss (%) | Final residue (%) | T <sub>95%</sub> |
|----------------|-------------------|----------------------|-------------------|----------------------|-------------------|------------------|
| DOP (1)        | 284               | 73.9                 | 452               | 15.9                 | 8.2               | 262              |
| DOTP (2)       | 296               | 73.7                 | 442               | 16.7                 | 8.3               | 278              |
| ESBO (5)       | 291               | 54.1                 | 447               | 34.5                 | 7.2               | 290              |
| MEEP (9)       | 266               | 61.8                 | 442               | 22.9                 | 13.8              | 261              |
| mPEG-ESBO (10) | 278               | 63.2                 | 450               | 23.6                 | 10.2              | 272              |
| MEFE (11)      | 277               | 61.5                 | 440               | 25.7                 | 11.8              | 240              |
| IEEP (12)      | 272               | 61.2                 | 439               | 25.3                 | 10.2              | 263              |

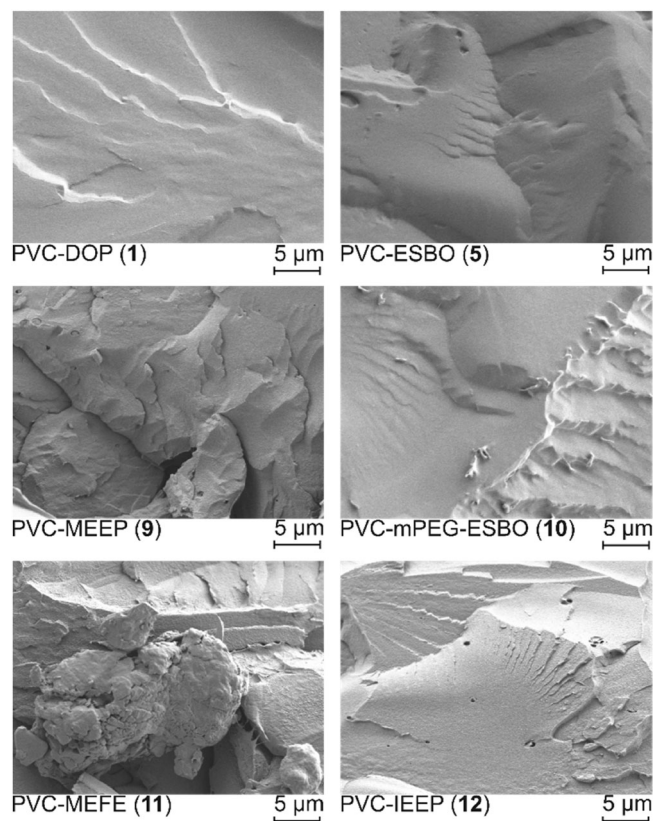


FIGURE 12 SEM images of cold fractured plasticised PVC sample surfaces, showing the effect of plasticizer on the morphology of the PVC-plasticizer blend.

as well as voids which could be caused by areas of plasticizer accumulation due to poor compatibility with PVC.

## 4 | CONCLUSIONS

Four derivatives of ESBO **5** were synthesized through epoxide ring opening reactions (and subsequent modification in the case of MEFE **11**). Analysis of these products showed that the epoxide ring opening reaction did

not go to completion, with typically 1–3 addition reactions occurring per ESBO molecule (of approximately 4–5 epoxide groups per molecule).

These products were evaluated as potential bio-based plasticisers for PVC compounding, with the aim of matching the performance of the petrochemical plasticizer DOP. mPEG-ESBO showed the greatest plasticising behavior as measured by  $T_g$  suppression and tensile properties. The tensile strength and elongation of PVC-mPEG-ESBO exceeds that of PVC-DOP. The other ESBO derivatives showed poor elongation at breakpoint, indicating that they do not plasticise the PVC chains effectively. IEEP and MEEP both showed delamination after molding which indicates poor compatibility of the plasticisers. The loss modulus peaks by DMA were also wider for all derivatives of ESBO, which can also indicate poor compatibility. The peaks for IEEP **12** were particularly irregularly shaped, suggesting that there may be multiple glass transitions due to phase separation in the material. mPEG functionalised ESBO has been shown to be a very promising candidate for the drop-in replacement of conventional petrochemical PVC plasticisers with a bio-based, non-toxic alternative which can be efficiently prepared from commercially available ESBO whilst substantially retaining some heat-stabilizing performance.

## AUTHOR CONTRIBUTIONS

**Katharine Burns:** Conceptualization (equal); investigation (lead); visualization (lead); writing – original draft (lead). **Ian D. V. Ingram:** Conceptualization (equal); investigation (supporting); supervision (lead); writing – review and editing (lead). **Johannes H. Potgieter:** Supervision (supporting); writing – review and editing (supporting). **Sanja Potgieter-Vermaak:** Supervision (supporting).

## ACKNOWLEDGMENTS

We would like to thank Hayley Andrews for her assistance with SEM imaging.

**CONFLICT OF INTEREST STATEMENT**


This work was funded by Alphagary Ltd., with whom K Burns was previously employed. Alphagary Ltd. had no further influence on the investigation or findings.

**DATA AVAILABILITY STATEMENT**

The raw data required to reproduce these findings are available to download from <https://doi.org/10.23634/MMU.00632240>.

**ORCID**

Katharine Burns  <https://orcid.org/0000-0002-8568-0580>

Ian D. V. Ingram  <https://orcid.org/0000-0002-3153-9637>

Johannes H. Potgieter  <https://orcid.org/0000-0003-2833-7986>

Sanja Potgieter-Vermaak  <https://orcid.org/0000-0002-1994-7750>

**REFERENCES**

- [1] L. M. De Espinosa, A. Gevers, B. Woldt, M. Grass, M. A. R. Meier, *Green Chem.* **2014**, *16*, 1883.
- [2] M. Bocque, C. Voirin, V. Lapinte, S. Caillol, J. J. Robin, *J. Polym. Sci., Part A: Polym. Chem.* **2016**, *54*, 11.
- [3] M. G. A. Vieira, M. A. Da Silva, L. O. Dos Santos, M. M. Beppu, *Eur. Polym. J.* **2011**, *47*, 254.
- [4] I. A. Sheikh, M. A. Beg, *Reprod. Toxicol.* **2019**, *83*, 46.
- [5] U. Wirnitzer, U. Rickenbacher, A. Katerkamp, A. Schachtrupp, *Toxicol. Lett.* **2011**, *205*, 8.
- [6] F. Chiellini, M. Ferri, A. Morelli, L. Dipaola, G. Latini, *Prog. Polym. Sci.* **2013**, *38*, 1067.
- [7] G. Wypych, *PVC Formulary*, 2nd ed., ChemTec Publishing, ON, Canada **2015**.
- [8] K. Burns, J. H. Potgieter, S. Potgieter-Vermaak, I. D. V. Ingram, C. M. Liauw, *J. Appl. Polym. Sci.* **2023**, *140*, e54104.
- [9] A. Guo, Y. J. Cho, Z. S. Petrovic, *J. Polym. Sci., Part A: Polym. Chem.* **2000**, *38*, 3900.
- [10] B. Dahlke, S. Hellbardt, M. Paetow, W. H. Zech, *J. Am. Oil Chem. Soc.* **1995**, *72*, 349.
- [11] G. Knothe, J. Krahl, J. V. Gerpen, *6.7 Soybean Oil Composition for Biodiesel, Biodiesel Handbook*, 2nd ed., AOCS Press, Urbana, IL, **2010**, p. 248.
- [12] R. Turco, R. Tesser, R. Vitiello, V. Russo, S. Andini, M. Di Serio, *Catalysts* **2017**, *7*, 309.
- [13] B. Lin, L. T. Yang, H. H. Dai, A. H. Yi, *J. Am. Oil Chem. Soc.* **2008**, *85*, 113.

- [14] L. C. Bailosky, L. M. Bender, D. Bode, R. A. Choudhery, G. P. Craun, K. J. Gardner, C. R. Michalski, J. T. Rademacher, G. J. Stella, D. J. Telford, *Prog. Org. Coat.* **2013**, *76*, 1712.
- [15] B. Zhong, C. Shaw, M. Rahim, J. Massingill, *J. Coat. Technol.* **2001**, *73*, 53.
- [16] H. H. Dai, L. T. Yang, B. Lin, C. S. Wang, G. Shi, *J. Am. Oil Chem. Soc.* **2009**, *86*, 261.
- [17] Y. F. Ma, F. Song, J. Yu, N. N. Wang, P. Y. Jia, Y. H. Zhou, *J. Polym. Environ.* **2022**, *30*, 2099.
- [18] P. Karmalm, T. Hjertberg, A. Jansson, R. Dahl, *Polym. Degrad. Stab.* **2009**, *94*, 2275.
- [19] B. Mehta, M. Kathalewar, A. Sabnis, *Polym. Int.* **2014**, *63*, 1456.
- [20] C. S. Coughlin, K. A. Mauritz, R. F. Storey, *Macromolecules* **1991**, *24*, 1526.
- [21] R. Bielski, G. Gryniewicz, *Green Chem.* **2021**, *23*, 7458.
- [22] K. J. Zeitsch, *The Chemistry and Technology of Furfural and its Many By-Products*, Elsevier, Amsterdam **2000**.
- [23] B. M. Lee, J. Jung, H. J. Gwon, T. S. Hwang, *J. Polym. Environ.* **2022**. <https://doi.org/10.21203/rs.3.rs-1275145/v1>
- [24] L. Chen, C. Sheng, Y. Duan, J. Zhang, *Polym.-Plast. Technol. Eng.* **2011**, *50*, 412.
- [25] Z. He, Y. Y. Lu, C. Q. Lin, H. H. Jia, H. L. Wu, F. Cao, P. K. Ouyang, *Polym. Test.* **2020**, *91*, 106793.
- [26] J. Tan, B. Liu, Q. Fu, L. Wang, J. Xin, X. Zhu, *Polymer* **2019**, *11*, 779.
- [27] A. Campanella, L. M. Bonnaillie, R. P. Wool, *J. Appl. Polym. Sci.* **2009**, *112*, 2567.
- [28] M. Rose, R. Palkovits, *ChemSusChem* **2012**, *5*, 167.
- [29] P. H. Daniels, A. Cabrera, *J. Vinyl Addit. Technol.* **2015**, *21*, 7.
- [30] D. T. C. Ang, Y. K. Khong, S. N. Gan, *J. Vinyl Addit. Technol.* **2016**, *22*, 80.
- [31] Y. Yang, J. C. Huang, R. Y. Zhang, J. Zhu, *Mater. Des.* **2017**, *126*, 29.
- [32] H. Pi, Y. Xiong, S. Y. Guo, *Polym.-Plast. Technol. Eng.* **2005**, *44*, 275.
- [33] W. H. Starnes, *Prog. Polym. Sci.* **2002**, *27*, 2133.

**SUPPORTING INFORMATION**

Additional supporting information can be found online in the Supporting Information section at the end of this article.

**How to cite this article:** K. Burns, I. D. V. Ingram, J. H. Potgieter, S. Potgieter-Vermaak, *J. Appl. Polym. Sci.* **2023**, e54656. <https://doi.org/10.1002/app.54656>